STATUS OF THE WOUND CONDUCTOR TASK

D. Pulikowski, P. Ebermann, F. Wolf, J. Fleiter, D. Tommasini, C. Scheuerlein, D. Schoerling, F. Lackner

CERN (TE-MSC, EN-MME, TE-CRG)

FCC Week, Amsterdam, 9th of April, 2018

CHARACTERIZATION OF Nb_3Sn WOUND CONDUCTOR

Irreversible degradation

- Quantify irreversible degradation of the conductor during the magnet assembly at RT
- Develop knowledge about stress distribution on Rutherford cable stack under the transversal load

Windability

- Development of winding test setup to define a “windability factor” allowing comparison between different Rutherford cables
- Development of adequate scanning method to quantify strand displacements during the winding process

Material characterization

- Improving knowledge of magnet material parameters for refinement of analytical design study and FE modelling
- Impact of thermal expansion on coil stiffness
- Thermal expansion of Rutherford cables during the reaction heat treatment

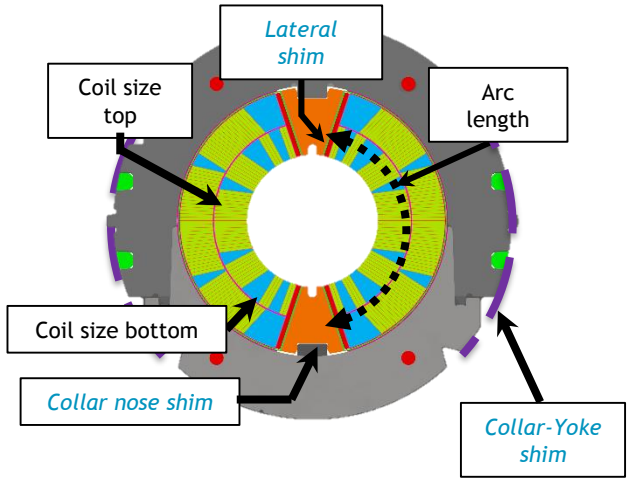

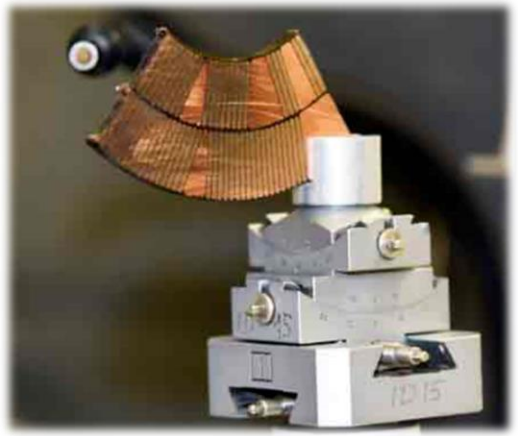

I_C DEGRADATION AFTER TRANSVERSAL PRESSURE AT RT

- The dominating load case in accelerator magnets is **transverse compressive**
- Coils are **loaded during the assembly, cooling, powering, quenching & thermal cycles**
- Experimental results about the room temperature (RT) stress limits of Nb_3Sn wires, cables and coils at which **irreversible conductor degradation** occurs are lacking
- The ongoing experiment aims to determine the **critical RT transverse compressive stress limits of cured, reacted and impregnated Nb_3Sn coil components**
- The degradation is quantified in terms of **critical current and n-value**

This work is carried out within an ongoing FCC-PhD. Collaboration with MSC-SCD, and profound academic supervision from the ATI (TU WIEN) as well as the work carried out from EN-MME and the USTEM (TU WIEN)

TESTING SEQUENCE

- The critical current of a reacted and impregnated two stack cable sample is measured in applied field in a high test current facility (FRESCA)
- Sample is taken out from FRESCA and compressed in a controlled manner at ambient temperature
- The sample is re-measured in FRESCA to check if, and by how much the compression has modified the I_C

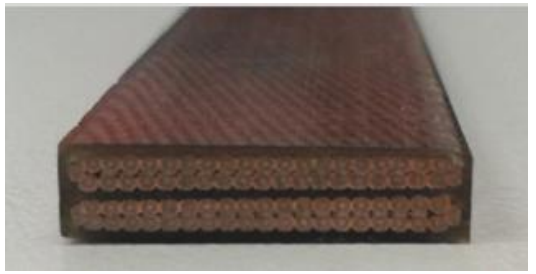

FRESCA sample, RRP – Nb_3Sn 11T cable stack

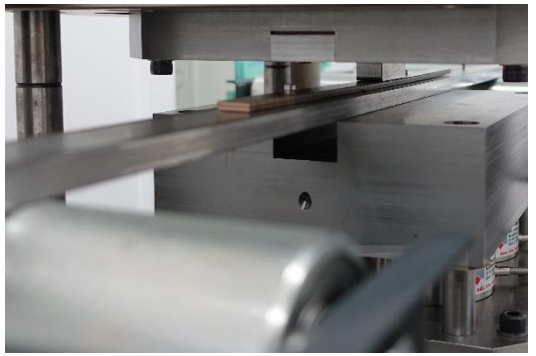

Cable compression on hydraulic press

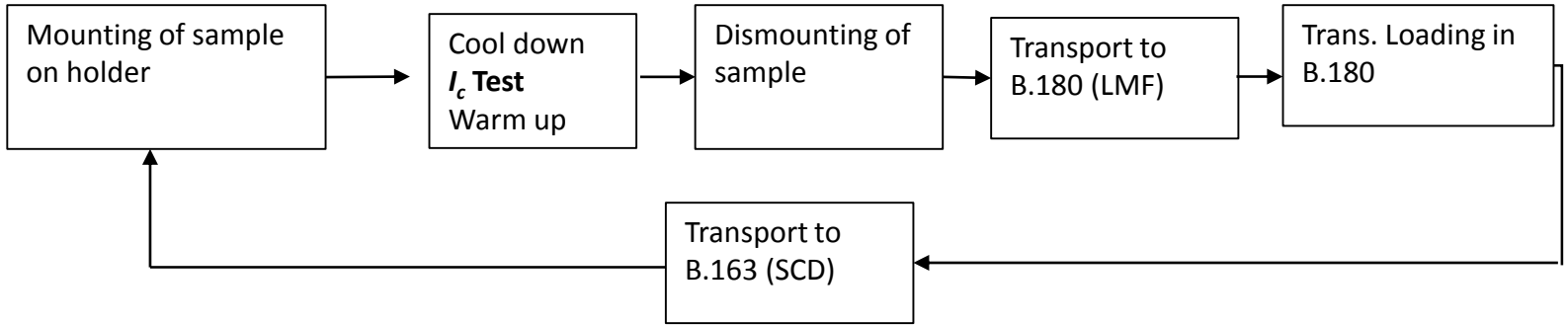

The test setup has been optimized in order ensure a known pressure distribution during the load step

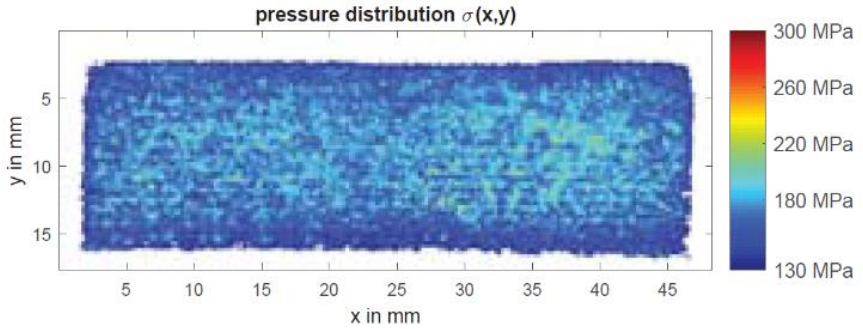

Improved knowledge on stress-distribution

I_c MEASUREMENT RESULTS OF FEASIBILITY SAMPLE

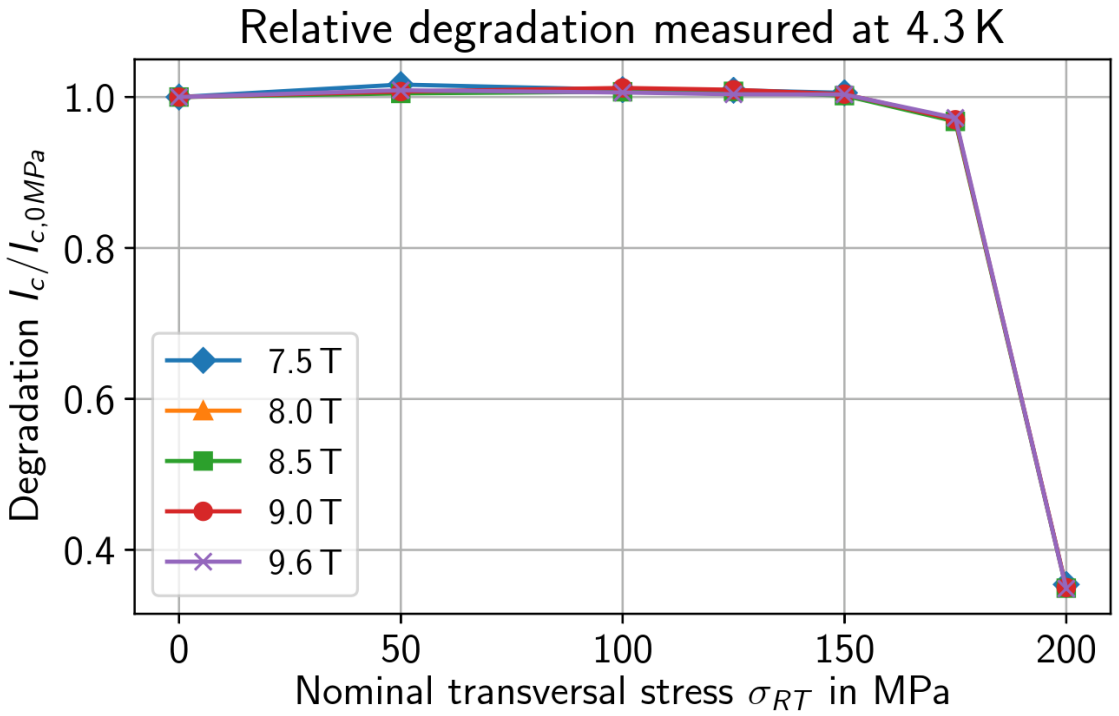

- Measured at 4.3 K and 1.9 K in FRESCA test station
- E_c = 3µV m^{-1}, dI/dt = 100 A s^{-1}, d=300 mm, $B_{self} \approx$ 80 mT(kA)$^{-1}$ I
- Correction of inductive offset and resistive part
- **Degradation of less than 4 % after 175 MPa**

P. Ebermann et al, „Irreversible degradation of Nb_3Sn Rutherford cables due to transverse compressive stress at room temperature“, SuST, accepted for publication

Status

- ❑ Feasibility study with 11T test cable (wire RRP127/169)
  - ❑ Measured up to 200 MPa in FRESCA test station incl. subsequent microscopy

Useful input for the collaring process of the HL-LHC 11T:

- ❑ 3 samples made of 11T series cables (wire RRP108/127)
  - ❑ Without mica (currently at RHT)
  - ❑ With standard mica geometry (**ongoing measured up to 125 MPa**)
  - ❑ With extended mica geometry (currently at impregnation)

Cable cross section

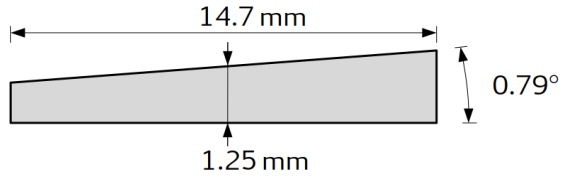

Sample cross section

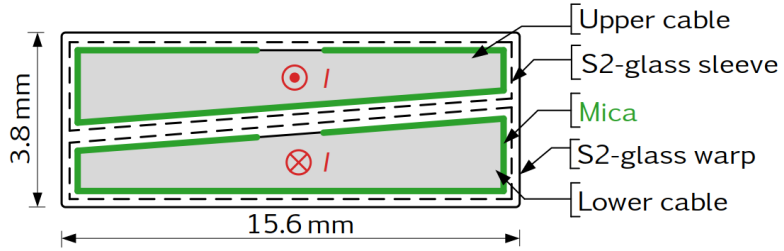

POST ANALYSIS – CRACK DETECTION

- Metallographic preparation and **SEM** observation
  - Longitudinal
  - Transversal
  - Entire etching with HNO_3

- Performed with
  - TU-WIEN (USTEM)
  - CERN (EN-MME)

- Ongoing work for analysis of
  - Cracks
  - Crack shape und surface
  - Crack density with digital image processing
  - Development of analytical and numerical model to predict imposed stress peaks leading to the observed crack patterns.

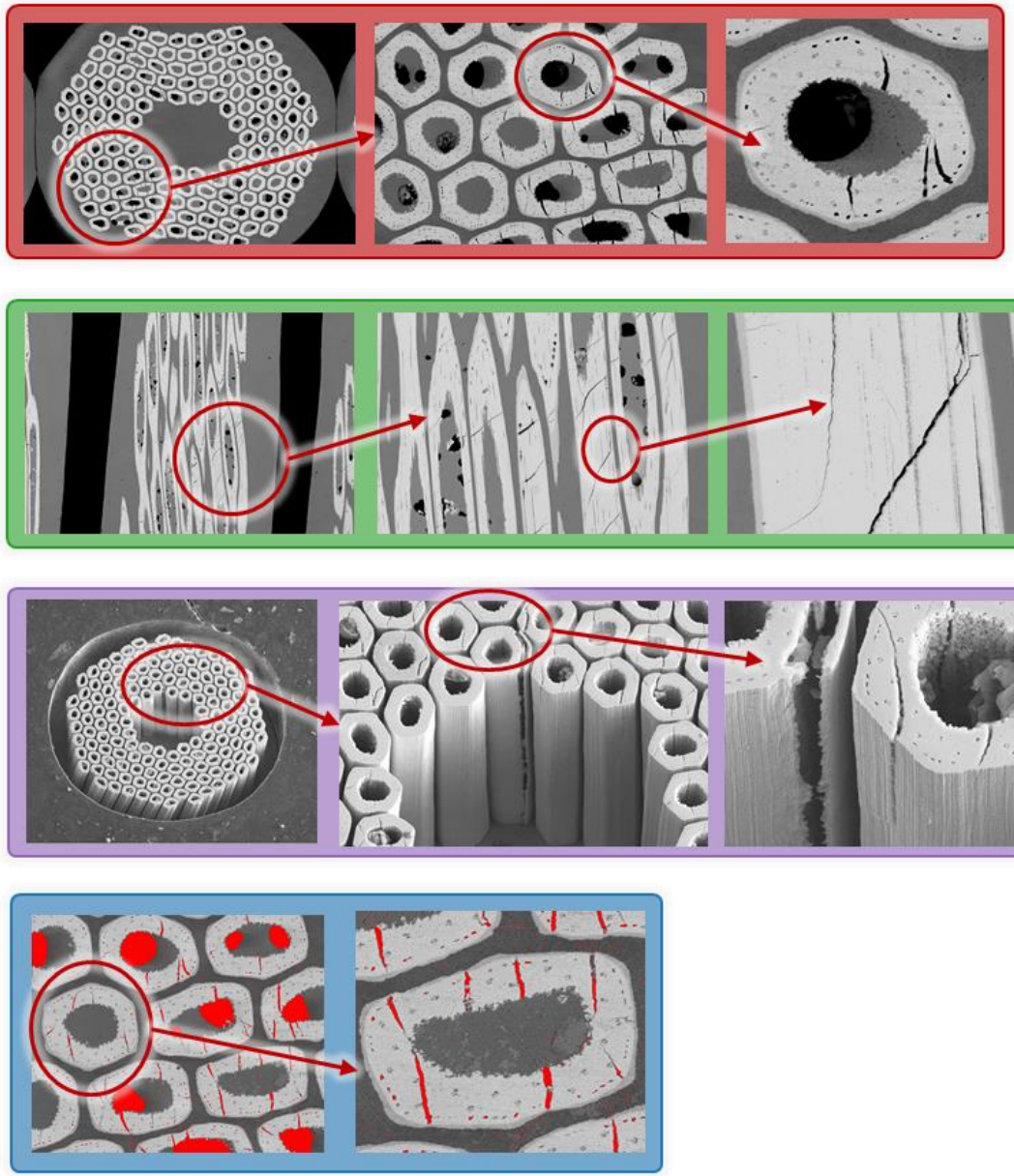

WINDABILITY

- Measure and model the geometrical evolution of cables during winding.
- Identification of the parameters dominating this process to possibly provide feedback for cabling & winding.
- Set-up a standard to quantify a “windability factor” or similar.

Rutherford cable behavior	Instability
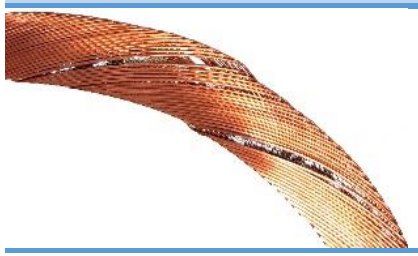	Opening
	Tightening
	Decabling
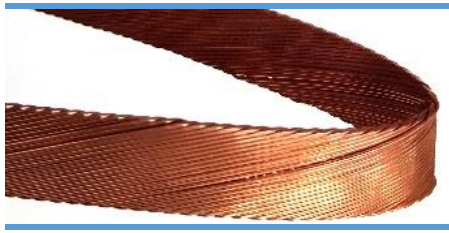	Strand pop-out

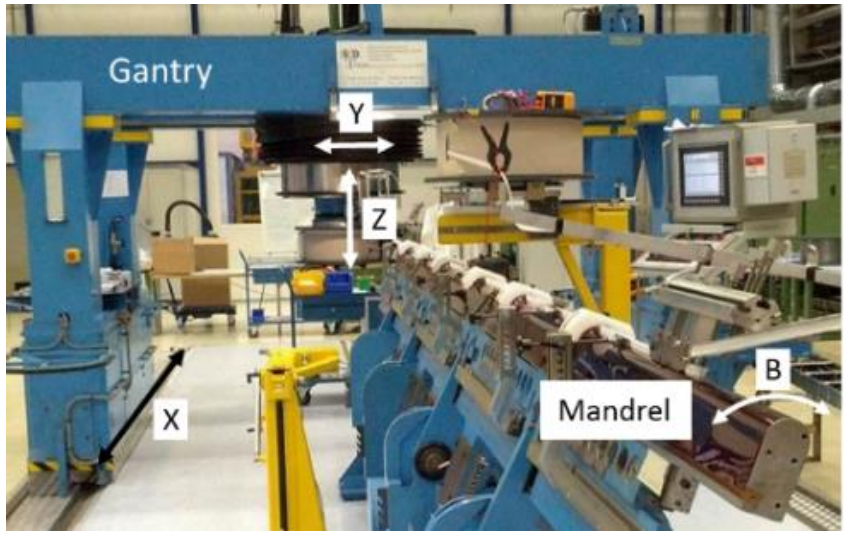

CERN-LMF, 11T dipole winding machine

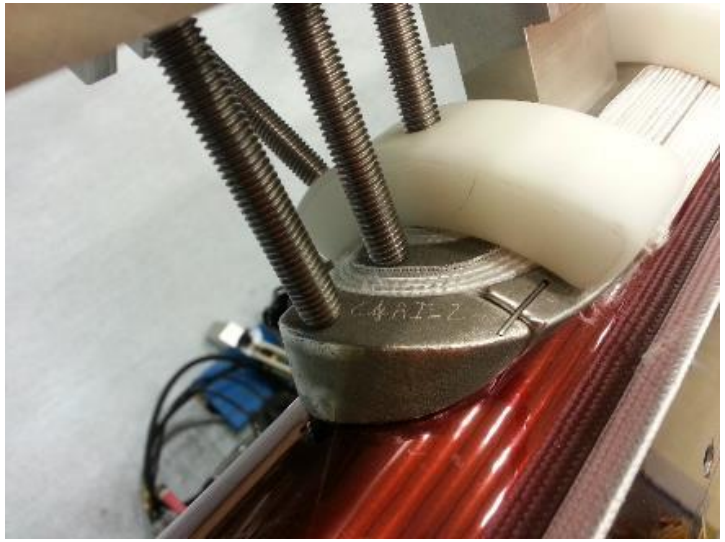

CERN-LMF, 11T dipole pole end

Courtesy of D. Pulikowski

WINDABILITY

Typical findings during the winding of Nb_3Sn coils

- ❑ Protrusion from the mandrel surface
- ❑ Strand pop-out

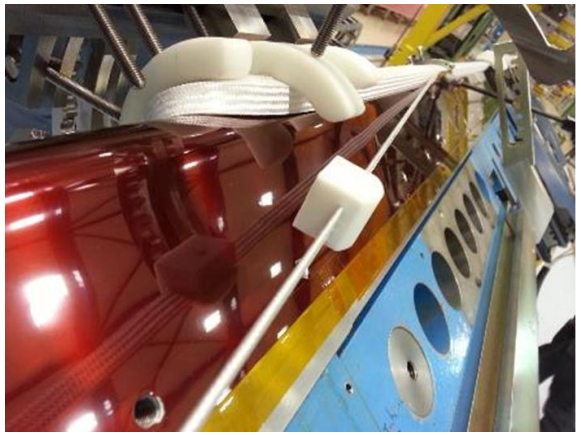

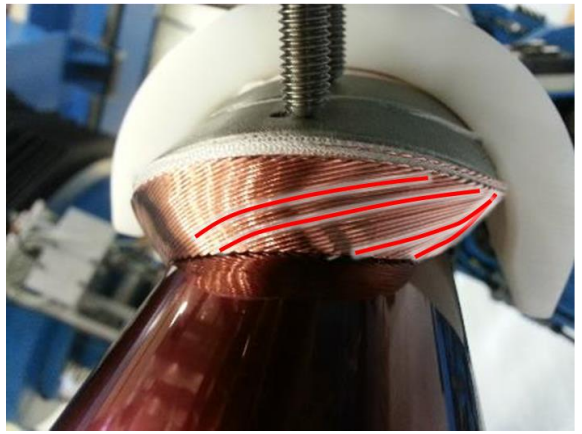
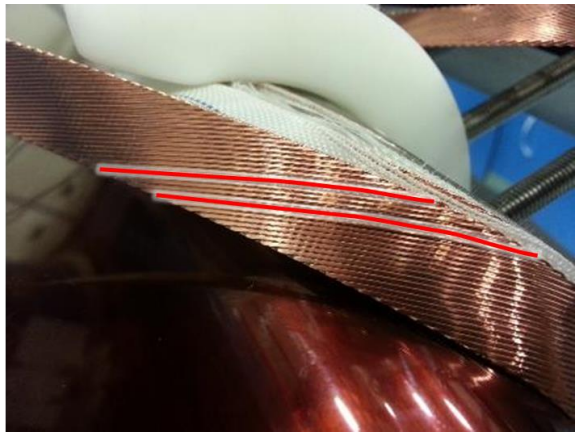

- ❑ Quantify geometrical displacements due to observed instabilities
- ❑ Proposal and definition of a “windability factor” allowing to compare results of different cable geometries

1 DEGREE OF FREEDOM (DOF) WINDING MOCKUP

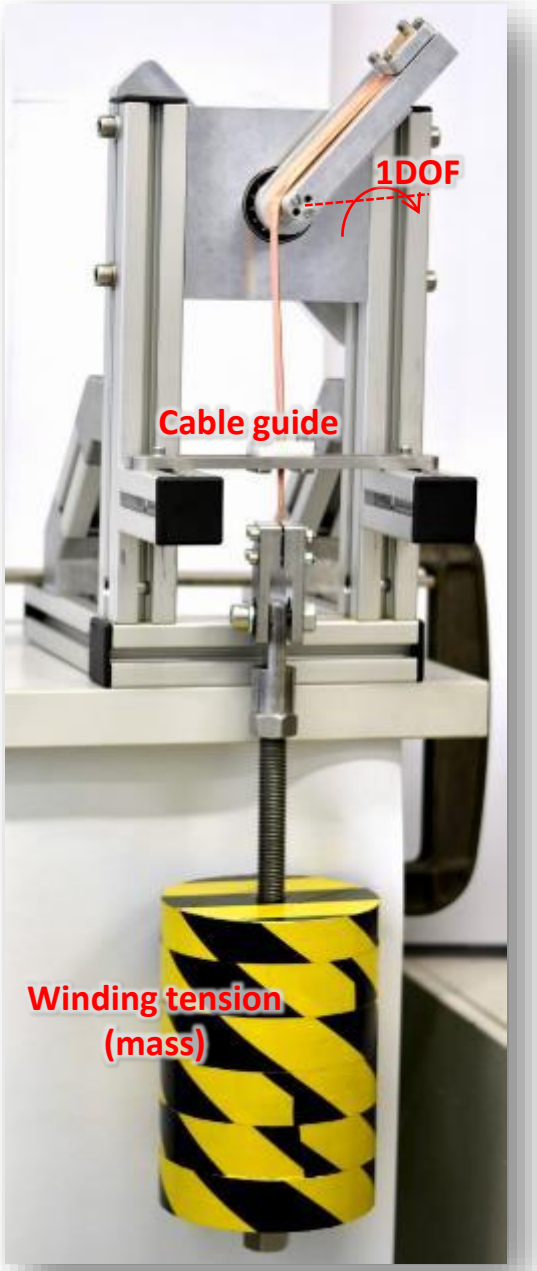

- Allows to wind specimens with the **Rutherford type cables in 1 DOF**
- Provides repeatable conditions;
- **Allows to adjust several winding parameters:**
  - Winding tension, Bending radius, Pretorsion, Cable guide position and angle & winding direction.

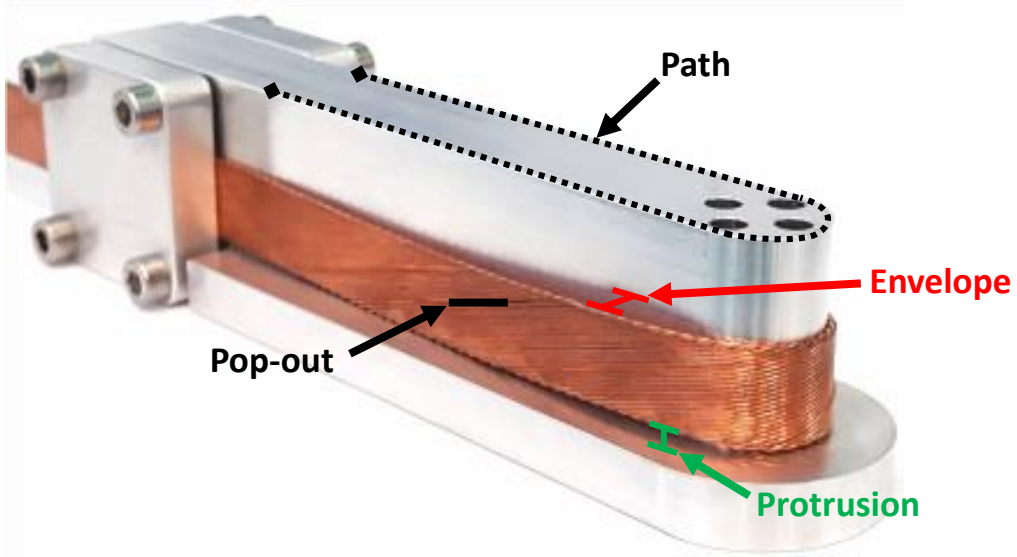

Sample holder for winding tests

1 DOF WINDING SCANNER

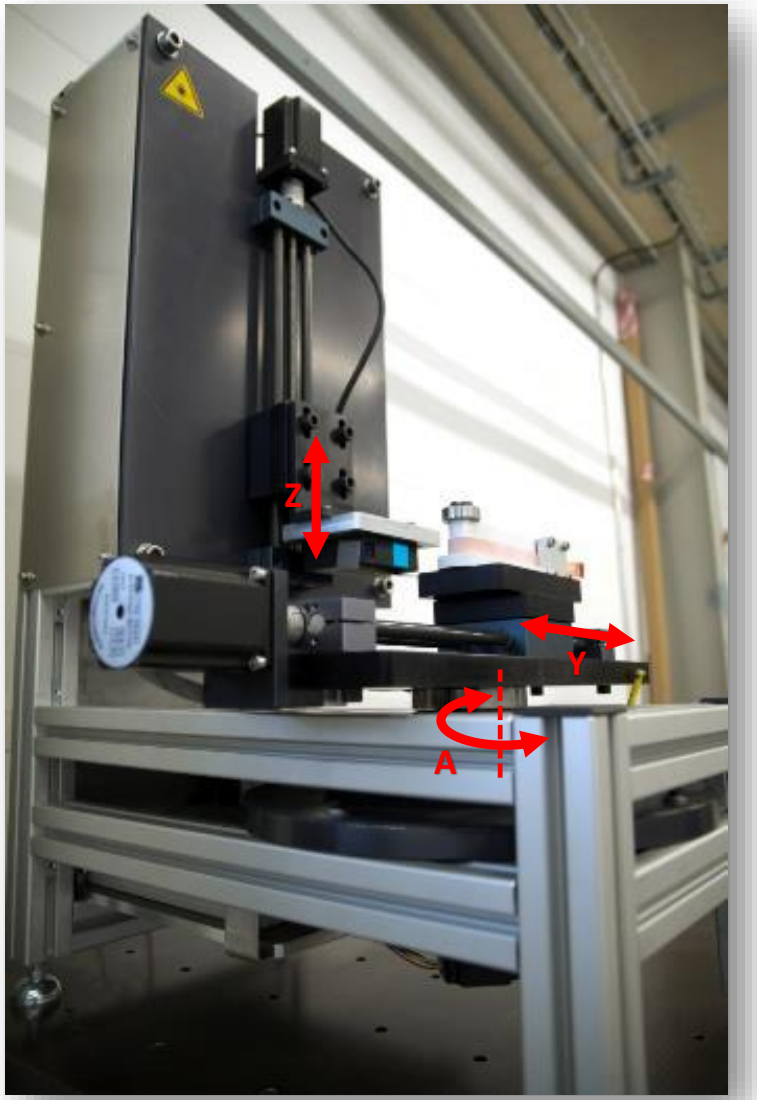

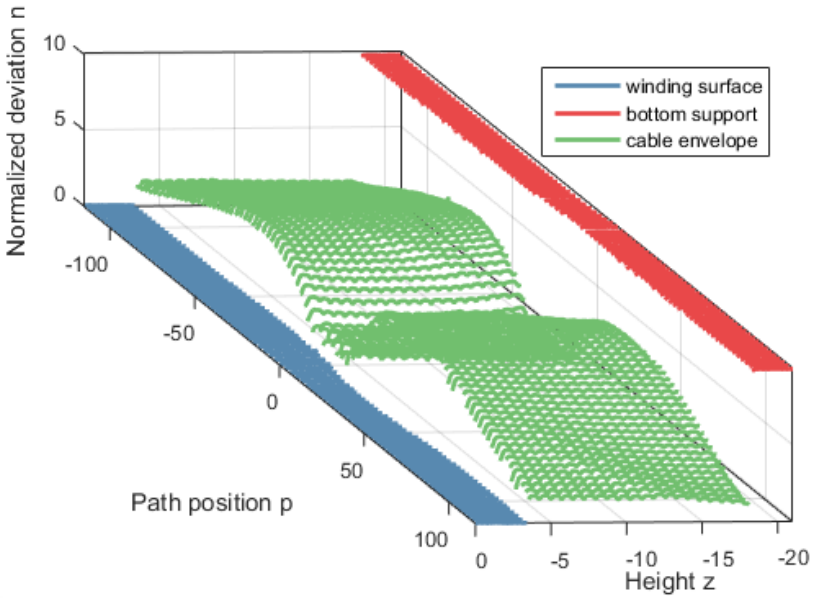

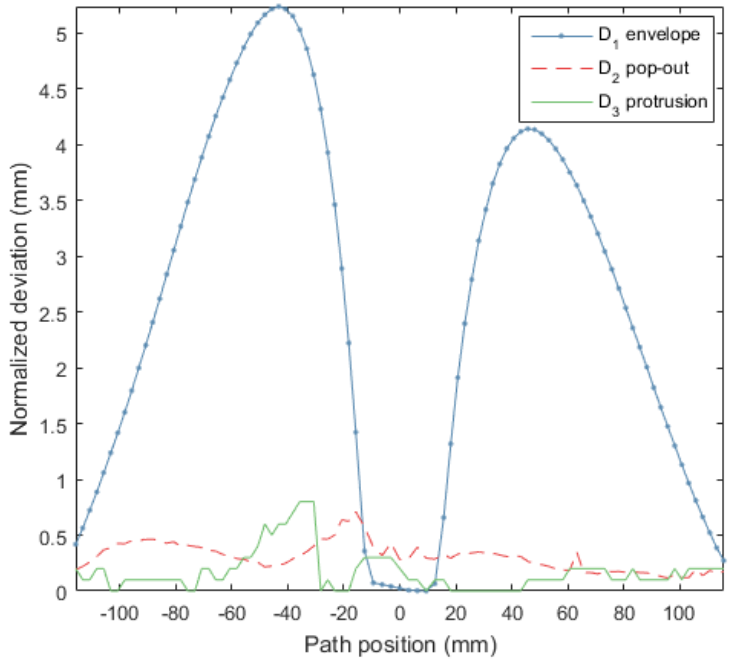

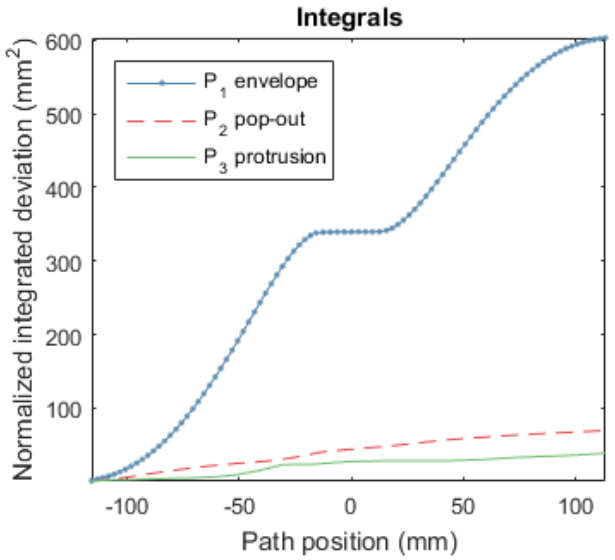

RESULTS FROM WINDING CAMPAIGNS

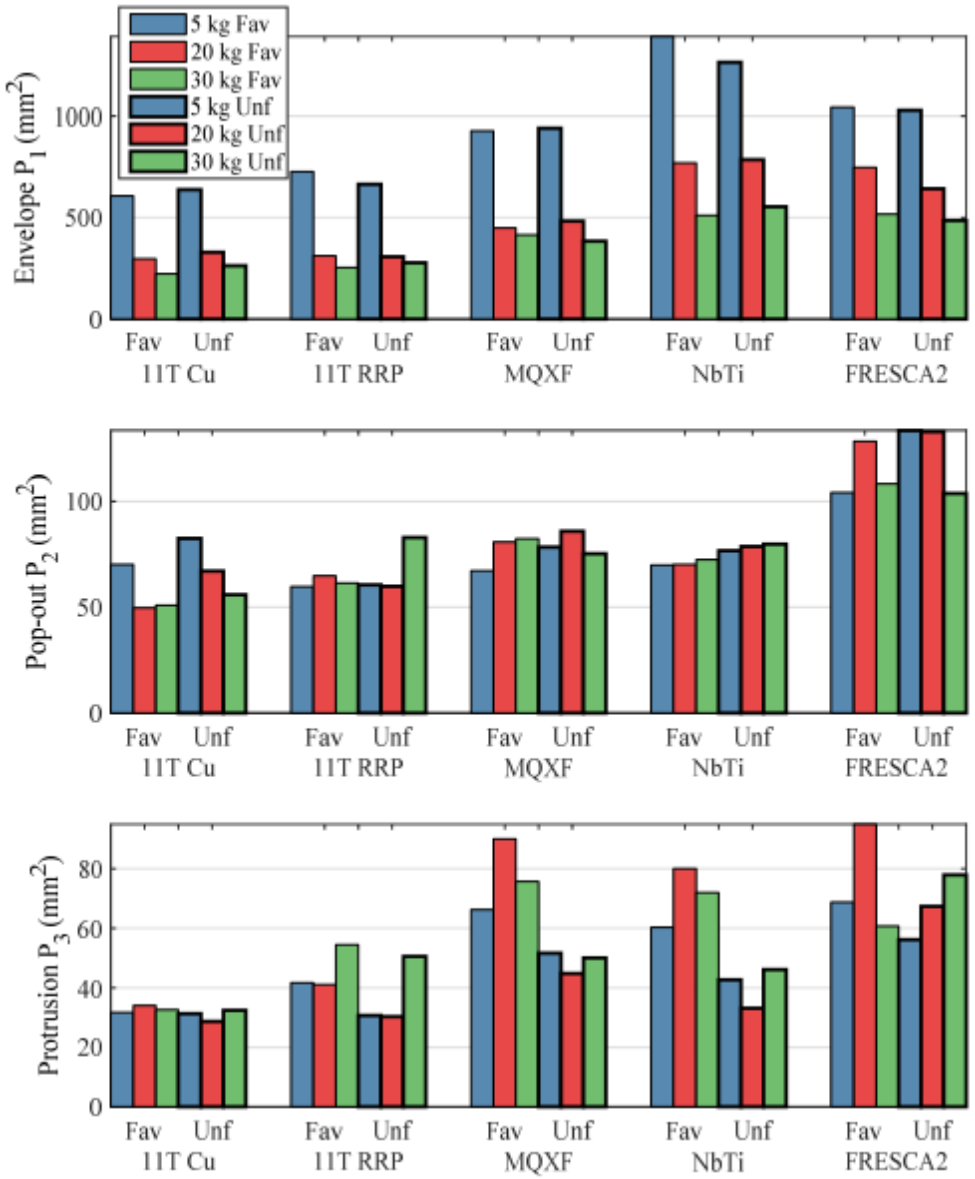

The average winding performance of three specimens wound with various winding mass and different winding direction.

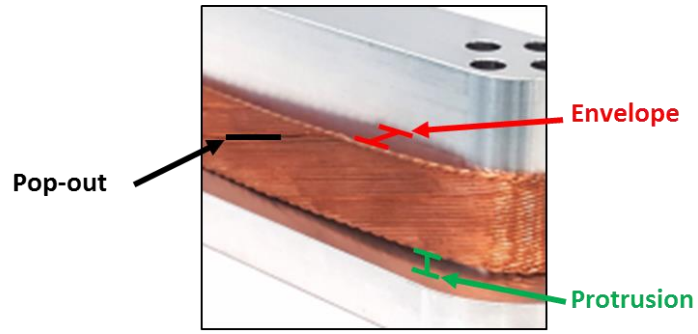

- With increased winding tension the envelope deformation is becoming smaller. No significant difference between various winding direction.
- Strand pop-out shows less dependence on the winding parameters, the deformation improvement is not as clear as for the envelope deformation. Small difference between the winding directions.
- The protrusion shows the largest dependence on the winding direction, exhibiting in average smaller values for the unfavourable direction.
- Depending on the deformation type, one can find different winding tension and direction providing the smallest values. Therefore the pre-torsion study was launched, aiming to investigate the improvement by introducing new parameter to the winding study.

APPLIED PRETORSION

Pre-torsion – maintaining the cable twist throughout the winding with use of the angular guide. Investigating the clockwise twist, i.e. tightening of the cable.

Investigating the winding process improvement due to the additional DOF

- Adjusting the cable torsion with the angular guide: 0°, 22.5°, 45°;
- The adjustment of the torsion angle improves the winding quality and performance.

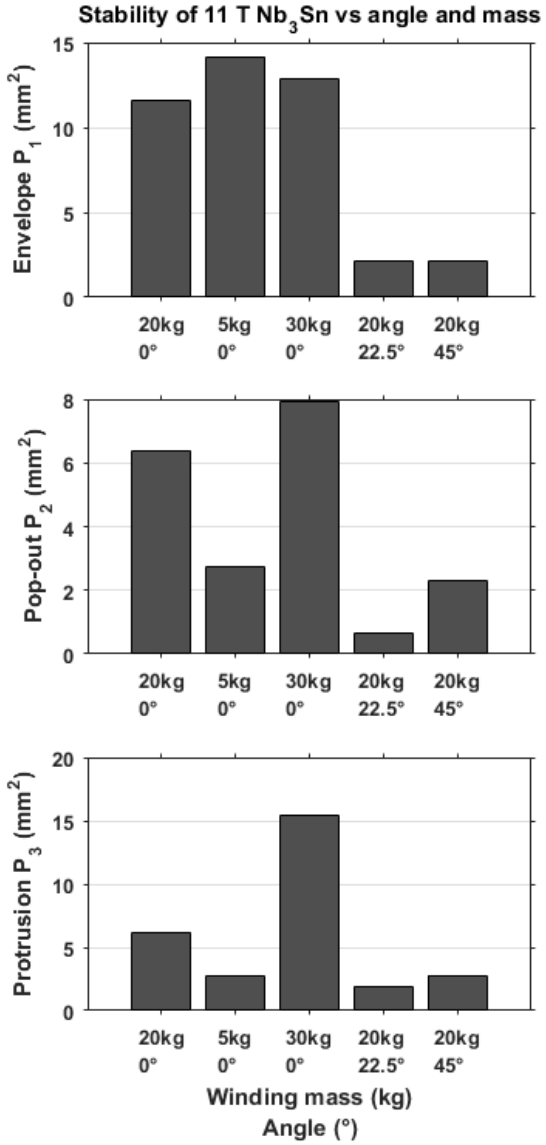

- *D. Pulikowski, F. Lackner et al., "Testing mechanical behavior of Nb_3Sn Rutherford cable during coil winding," IEEE Trans. Appiled Supercond., vol. 27, no. 4, 2017.*
- *D. Pulikowski, F. Lackner, C. Scheuerlein, and M. Pajor, "Numerical modelling of a superconducting coil winding process with Rutherford type Nb_3Sn cable," J. Mach. Constr. Maint., pp. 13–19, 2017.*
- *D. Pulikowski, F. Lackner, C. Scheuerlein, F. Savary, D. Tommasini, and M. Pajor, "Windability tests of Nb_3Sn Rutherford cables for HL-LHC and FCC," IEEE Trans. Appiled Supercond., vol. 28, no. 3, 2018.*

ADDITIONAL MEASUREMENTS DURING COIL PRODUCTION

Determining the position of the cable center in the longitudinal axis after winding with use of image analysis.

Improved QC allows observing the relative turn deviation between consecutive production steps

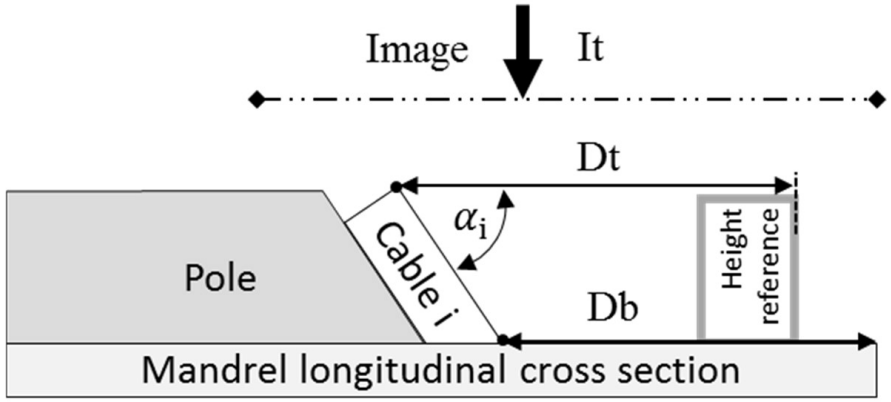

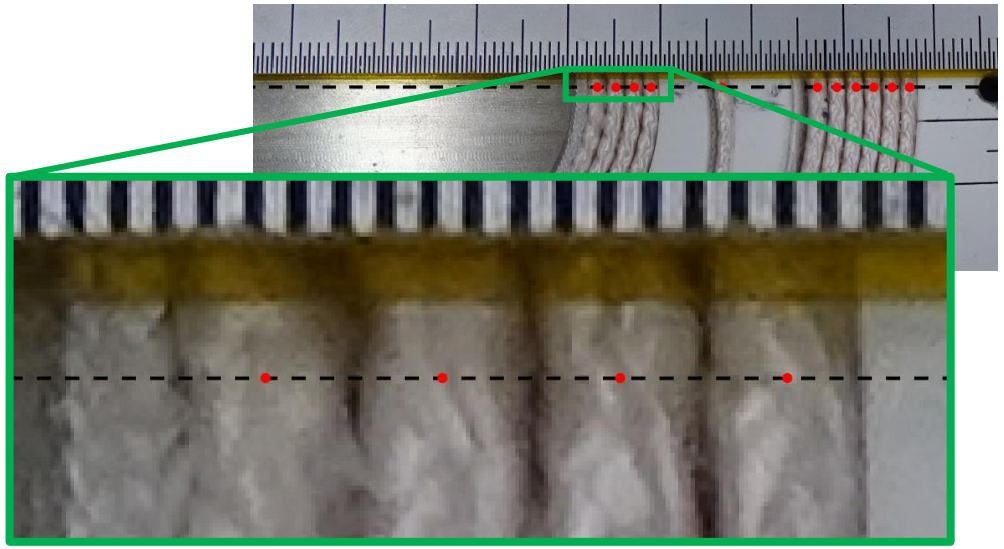

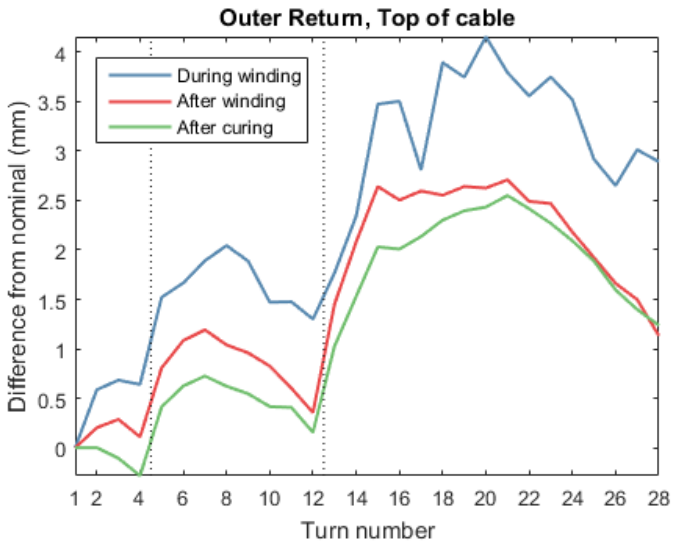

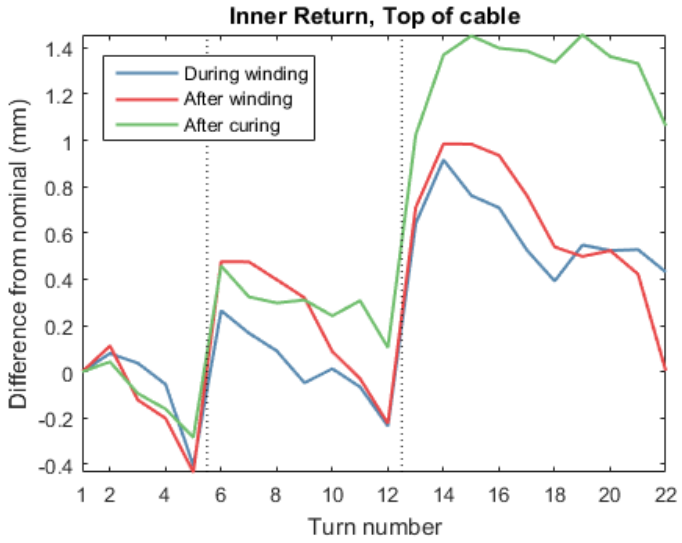

Additional work on mechanical properties:

- Magnet coil constituents
  - Static tensile and compression tests
  - Dynamic E-modulus and shear modulus tests
  - Thermal expansion measurements
  - Friction measurements
- Coil block stiffness

MECHANICAL PROPERTIES OF MAGNET CONSTITUENT MATERIALS

- Precise Young's moduli can be derived from static stress-strain measurements of materials that exhibit pronounced linear elastic behaviour (e.g. Ti6Al4V).
- The temperature dependence of the Young's modulus can be determined by dynamic resonance tests.

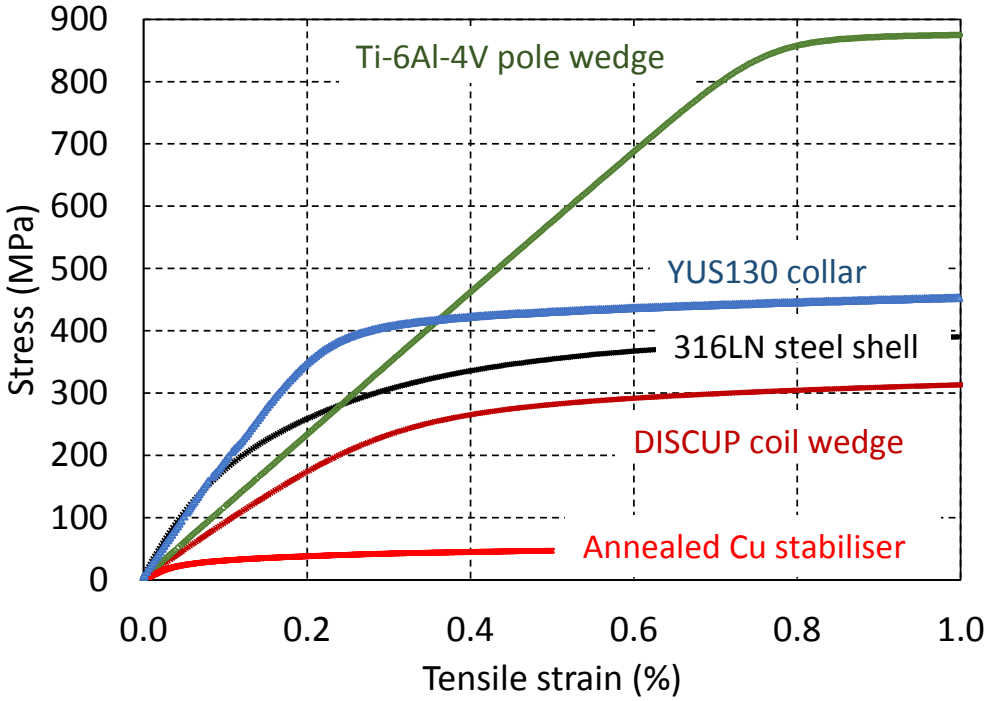

Comparison of the RT engineering stress-strain curves of different coil and magnet materials.

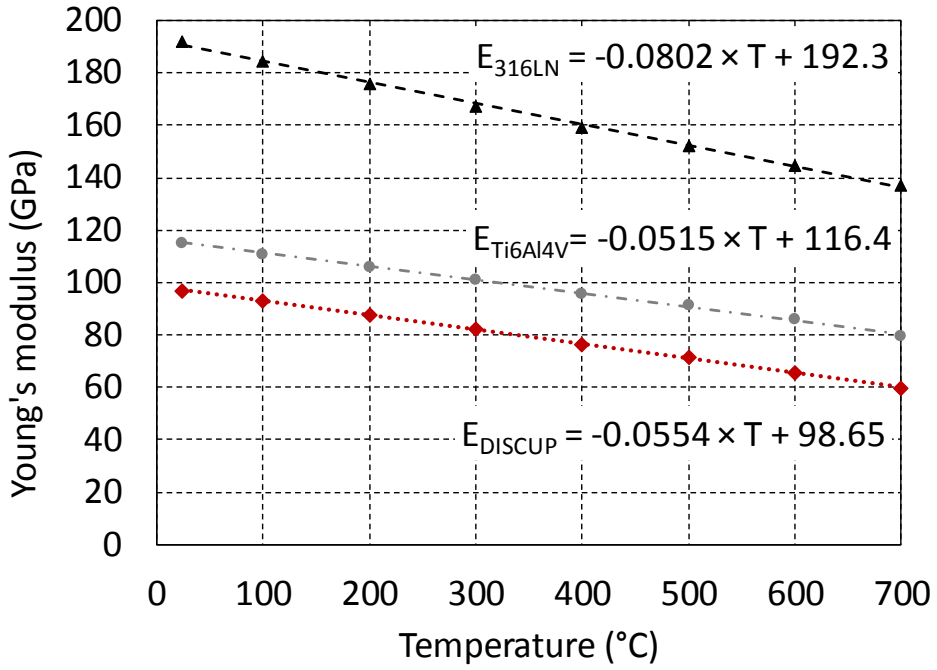

Temperature dependence of the DISCUP C3/30 coil wedge, Ti6Al4V pole wedge and 316LN stainless steel Young's moduli and linear fits.

- C. Scheuerlein, F. Lackner, F. Savary, B. Rehmer, M. Finn, P. Uhlemann, "*Mechanical properties of the HL-LHC 11 Tesla Nb_3Sn magnet constituent materials*", IEEE Trans. Appl. Supercond., 27(4), (2017), 4003007

TEMPERATURE DEPENDENT EXPANSION

Temperature dependent expansion of Nb_3Sn coil and magnet constituents:

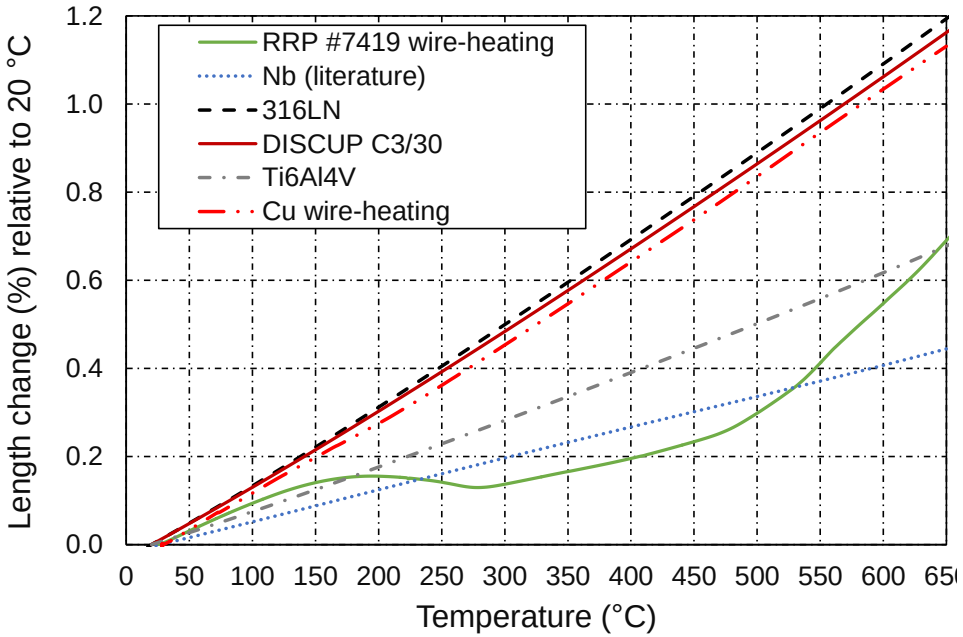

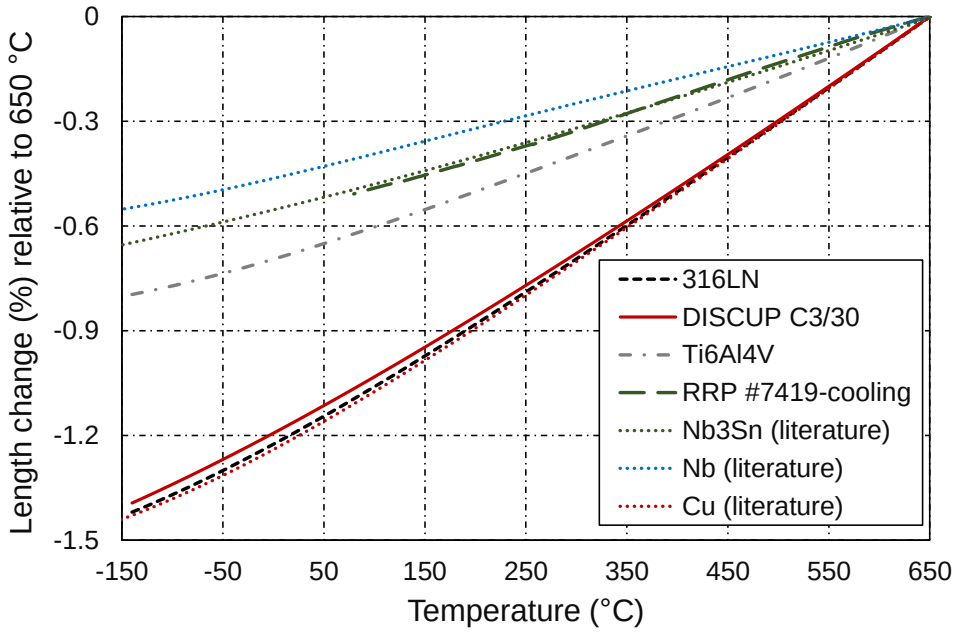

Relative length change of DISCUP C30/3, Ti6Al4V, 316LN and Nb3Sn RRP type wire during (a) first heating and (b) cool down from 650 °C. The thermal expansions of Cu, Nb and Nb_3Sn bulk are shown for comparison.

C. Scheuerlein, F. Lackner, F. Savary, B. Rehmer, M. Finn, C. Meyer, "Thermomechanical behavior of the HL-LHC 11 Tesla Nb_3Sn magnet coil constituents during reaction heat treatment", IEEE Trans. Appl. Supercond., 28(3), 2018, 4003806

FRICTION COEFFICIENTS

- At RT in air at a pressure of 100 MPa Ti6Al4V shows smooth and stable sliding against 316LN with a friction coefficient of ~0.4.
- At 4.2 K@100 MPa a strong stick-slip effect is observed, which could be one potential origin of magnet quenches.
- Application of the solid lubricant MoS_2 lowers the 4.2 K friction coefficient to about 0.08.
- In liquid He at 100 MPa Polyimide shows smooth and stable sliding against steel 316 LN with a friction coefficient of ~0.2.

Fig. 2. Samples: left: Ti6Al4V pads; right: steel 314LN cylinders

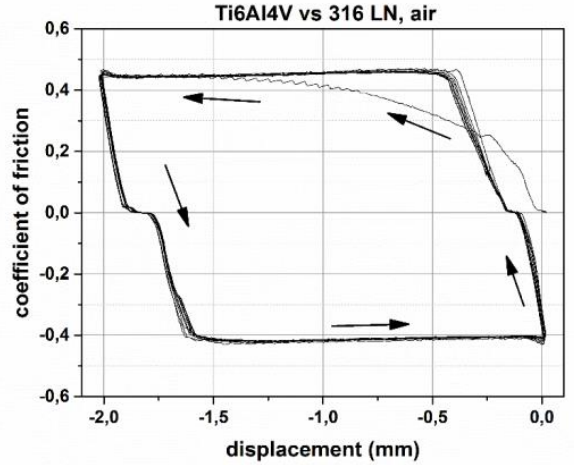

Fig. 3. Friction coefficient vs. displacement of Ti6Al4V against stainless steel 316LN in air at room temperature: smooth sliding, no static friction peak, no stick-slip

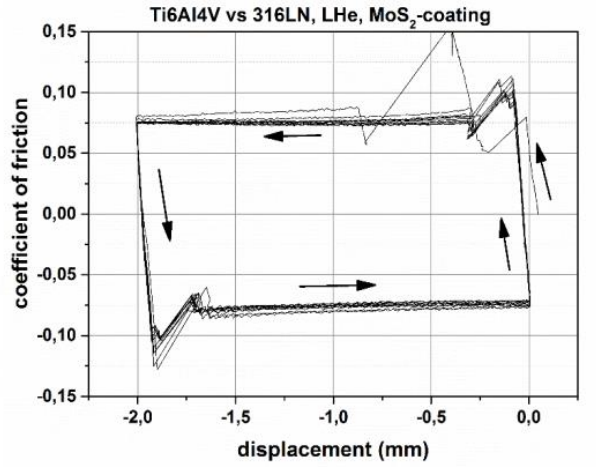

Fig. 5. Friction coefficient vs. displacement of Ti6Al4V with MoS2 coating against stainless steel 316LN in liquid helium (T = 4.2 K): smooth and stable sliding but distinct static friction peak

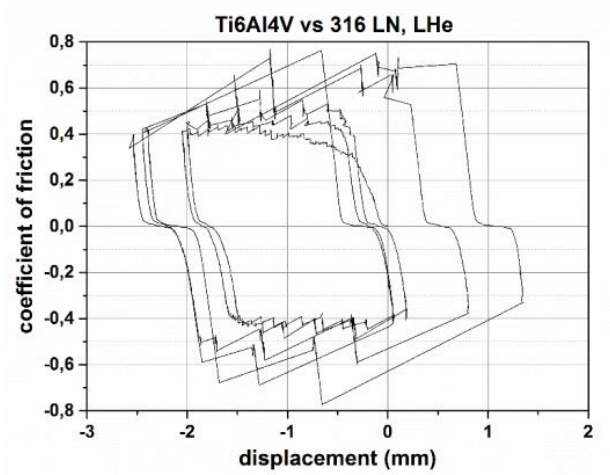

Fig. 4. Friction coefficient vs. displacement of Ti6Al4V against stainless steel 316LN in liquid helium (T = 4.2 K): strong stick-slip effect after the first friction cycle

T. Gradt, C. Scheuerlein, F. Lackner, F. Savary, "Friction-coefficient between the Ti6Al4V loading pole and the 316LN steel shims of the HL-LHC 11 T magnets", IEEE Trans. Appl. Supercond., 28(3), 2018, 10.1109/TASC.2018.2792469

TWO INDEPENDENT STRESS-STRAIN MEASUREMENT SET-UPS

Hydraulic test setup - CERN

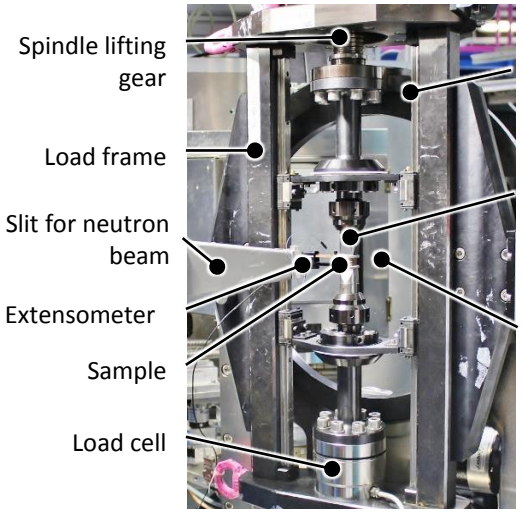

STRESS-SPEC setup at MLZ with 12 mm gauge length.

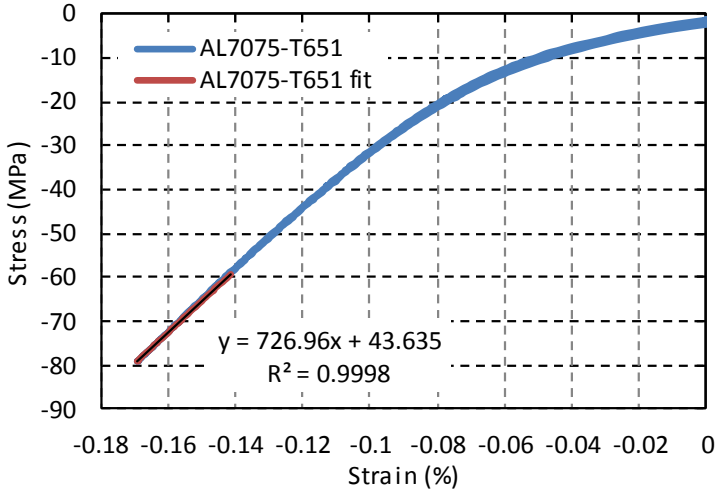

Reference measurement Al7075-T651((71.7 GPa) [2]

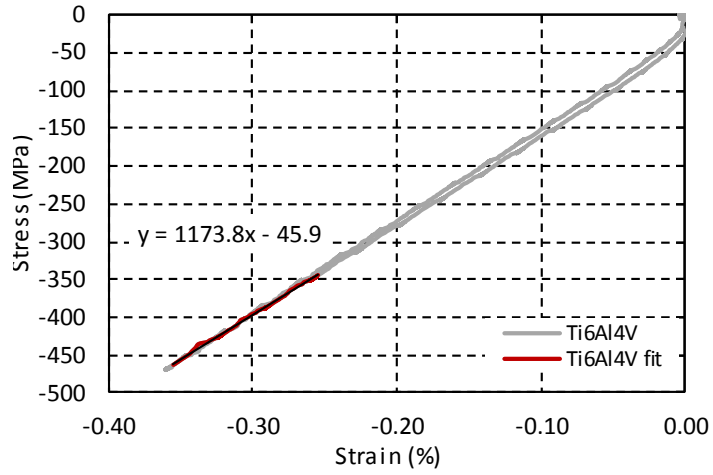

Reference measurement Ti6Al4V (116.7 GPa ±1GPa)

- Uncertainties caused by the compliance of the test set-ups avoided by using **extensometers** (**direct strain measurements**).
- All samples are made from **Nb_3Sn 11 T dipole Rutherford cable**, with **Mic**a and **S2 glass** insulation (cube, 15 mm).
- Ten-stack **samples reacted** in a dedicated mould, **three different levels of compaction**.
- 11 T dipole coil block sample machined from coil after cold test
- Impregnation (CTD-101K)
- **Non-impregnated** 11 T dipole ten-stack **sample** has been **tested for comparison**.

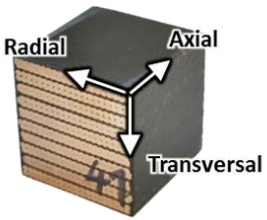

Ten stack

Coil segment

Non-imprg. ten stack

- *C. Scheuerlein et al., "Mechanical properties of the HL-LHC 11 Tesla Nb_3Sn magnet constituent materials," IEEE Trans. Appl. Supercond., vol. 27, no. 4, Jun. 2017.*
- *Charles Moosbrugger, Atlas of Stress-strain Curves, , ASM International 2nd Ed. 2002.*

STIFFNESS MEASUREMENTS - TEN STACKS (FIRST LOAD CYCLE)

Effect of transverse stress applied during reaction heat treatment on the stiffness of Nb_3Sn Rutherford cable stacks

- ❑ Stiffness comparison with respect to the compaction level (during RHT) due to clearance variation.
- ❑ Stiffness comparison for different load directions.

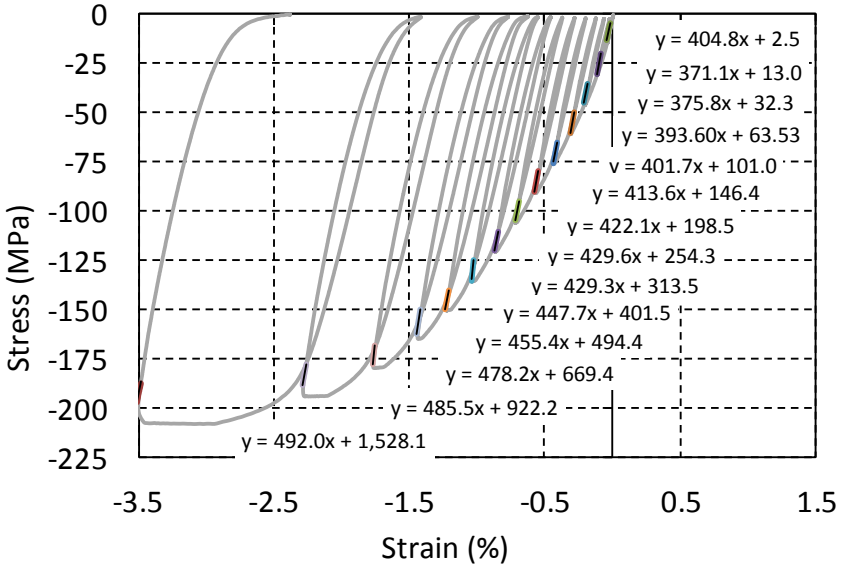

Transverse compressive stress-strain curve of the ten-stack sample reacted with the lowest compaction.

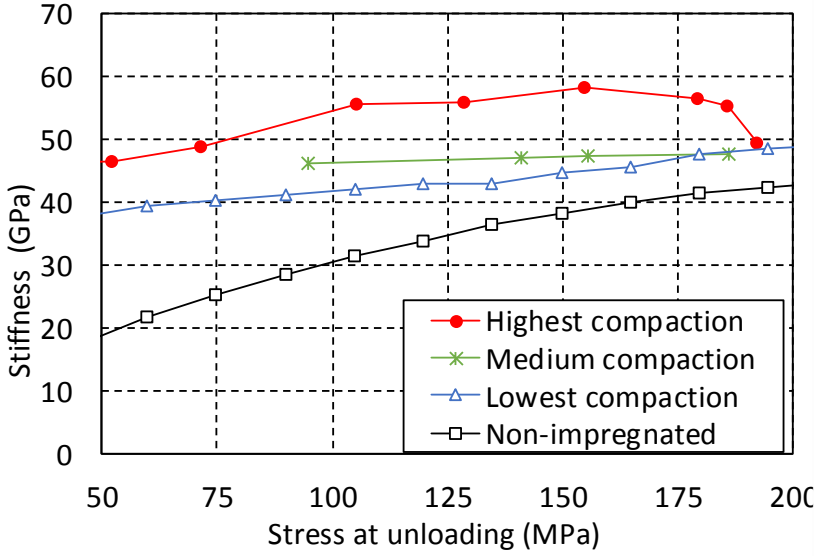

Stiffness comparison of different compaction levels due to clearance variation in the RHT mould. Non-impregnated stack reacted with lowest compaction.

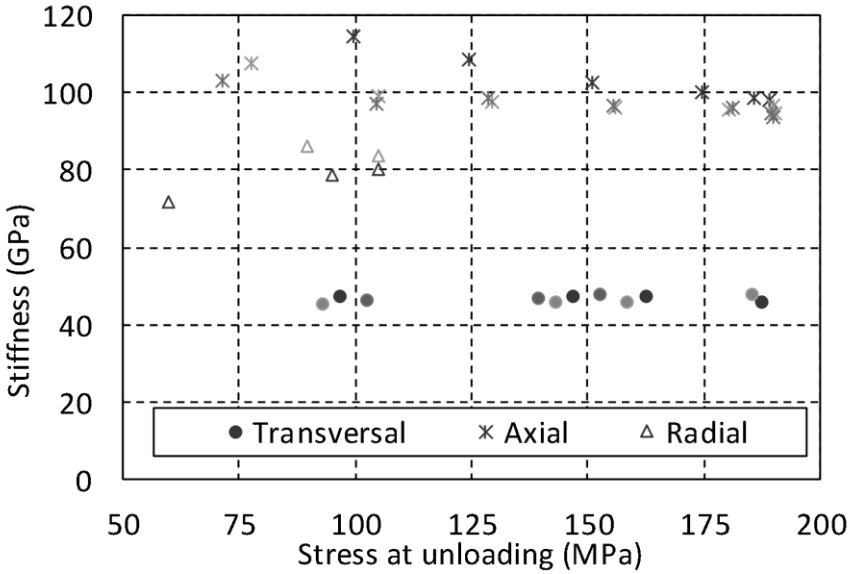

Stiffness in different sample directions, medium compaction during RHT

POSTER: 2AMSP32
F. Wolf: *Effect of transverse stress applied during reaction heat treatment on the stiffness of Nb_3Sn Rutherford cable stacks*

STIFFNESS OF COIL CONDUCTOR BLOCK VS. TEN STACK

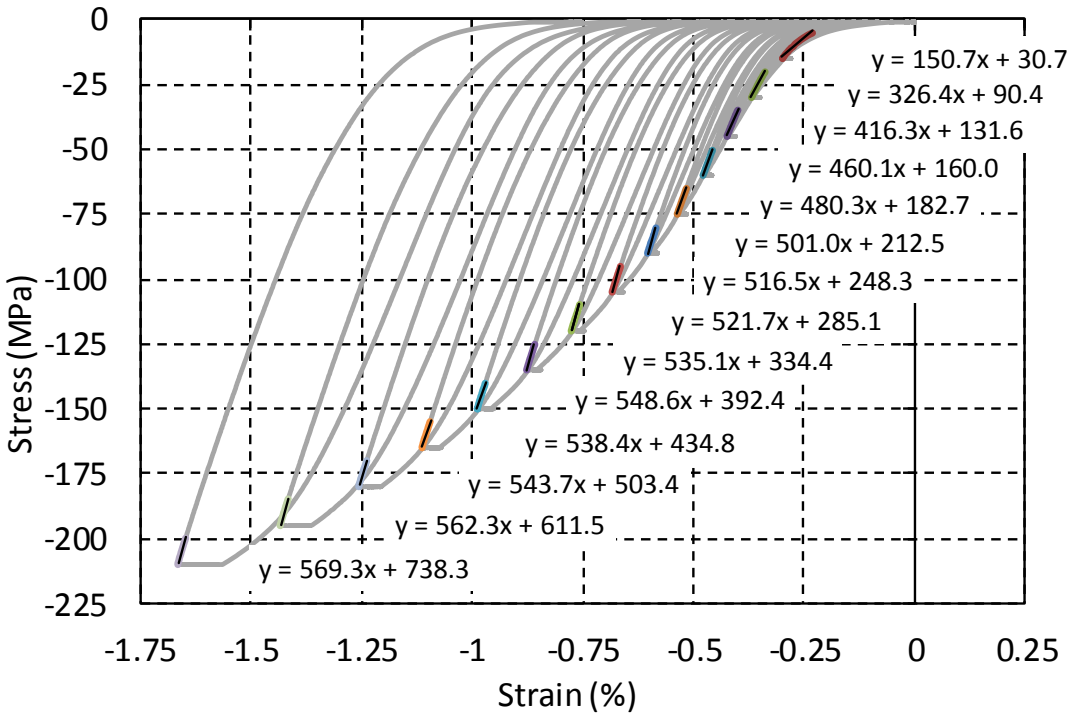

Compressive stress strain measurement of a coil segment, reloaded sample

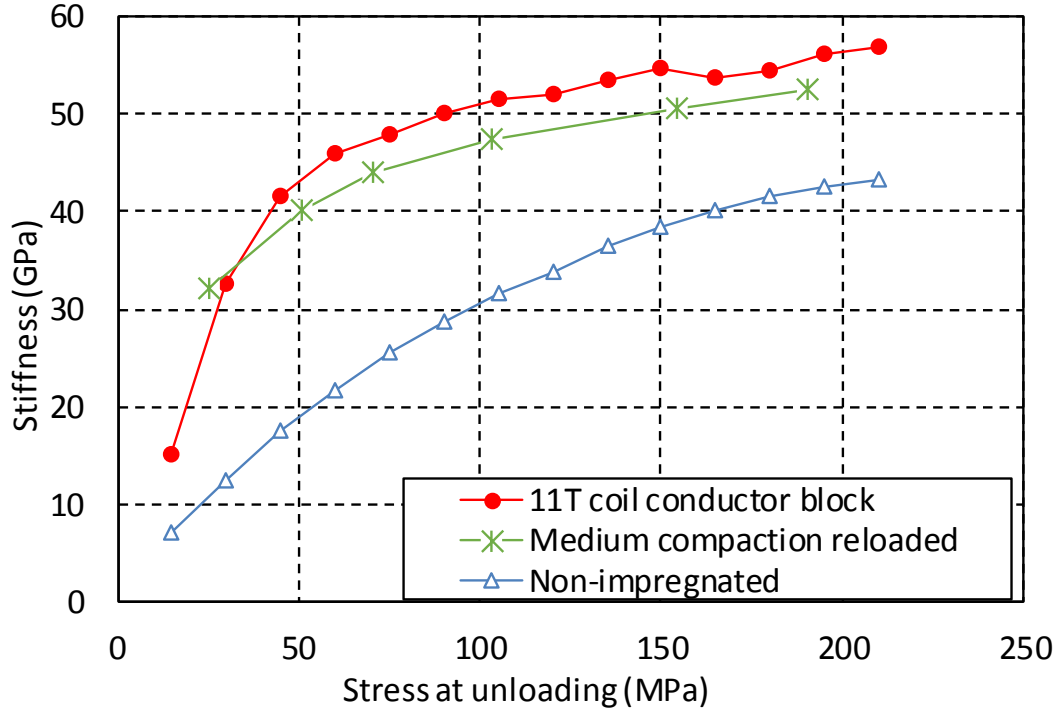

Stiffness comparison of impregnated and non impregnated cable stacks and a 11T coil conductor block.

- The transverse stiffness of the ten-stack samples with the medium compression during RHT matches well the 11 T dipole coil block stiffness.
- A strong creep behaviour is observed when the transversal load exceeds about 125 MPa.

POSTER: 2AMSP32
F. Wolf: *Effect of transverse stress applied during reaction heat treatment on the stiffness of Nb_3Sn Rutherford cable stacks*

CONCLUSIONS

- The results coming from the characterization of the irreversible cable degradation at RT, though very preliminary seem encouraging and support the choices performed within the EuroCirCol study and are of use within the HL-LHC coil fabrication.

- The winding setup may allow to define a windability factor useful for future cable development and winding process (robust and repeatable quality, production time).

- The effects of load direction, pre-compression during heat treatment and load history on the stiffness of Nb3Sn Rutherford cable blocks have been determined.

- A number of studies are under way to refine thermomechanical properties of magnet coil constituents as input parameters and meshes for FE analysis, and to predict the internal stress distribution in Nb_3Sn coils under different assembly and operating conditions.

PUBLICATIONS SINCE THE LAST FCC WEEK IN BERLIN

- D. Pulikowski, F. Lackner *et al.*, "Testing mechanical behavior of Nb_3Sn Rutherford cable during coil winding," *IEEE Trans. Appiled Supercond.*, vol. 27, no. 4, 2017.
- D. Pulikowski, F. Lackner, C. Scheuerlein, and M. Pajor, "Numerical modelling of a superconducting coil winding process with Rutherford type Nb_3Sn cable," *J. Mach. Constr. Maint.*, pp. 13–19, 2017.
- D. Pulikowski, F. Lackner, C. Scheuerlein, F. Savary, D. Tommasini, and M. Pajor, "Windability tests of Nb_3Sn Rutherford cables for HL-LHC and FCC," *IEEE Trans. Appiled Supercond.*, vol. 28, no. 3, 2018.
- F. Wolf, P. Ebermann, F. Lackner, D. Mosbach, Ch. Scheuerlein, K. Schladitz, D. Schoerling, "Characterization of the stress distribution on Nb_3Sn Rutherford cables under transverse compression", IEEE Trans. Appl. Supercond., vol. 28, no. 3, 8400106, 2018.
- F. Wolf, F. Lackner, M. Hofmann, C. Scheuerlein, D. Schoerling, D. Tommasini, "Effect of impregnation on the stiffness of Nb_3Sn coil segments and cable stacks," IEEE Trans. Appl. Supercond., To be submitted for publication in 2018.
- P. Ebermann, J. Fleiter, O. Kalouguine, F. Lackner, C. Scheuerlein, D. Schoerling, D. Tommasini, F. Wolf and M. Eisterer, "Characterization of irreversible degradation of Nb_3Sn Rutherford cables due to transversal compression stress at room temperature", Superconductor Science and Technology, Submitted for publication in 2018.
- C. Scheuerlein et al., "Mechanical properties of the HL-LHC 11 Tesla Nb_3Sn magnet constituent materials", IEEE Trans. Appl. Supercond., vol. 27, no. 4, Jun. 2017, Art. no. 4003007.
- C. Scheuerlein, F. Lackner, F. Savary, B. Rehmer, M. Finn, C. Meyer, "*Thermomechanical behavior of the HL-LHC 11 Tesla Nb_3Sn magnet coil constituents during reaction heat treatment*", IEEE Trans. Appl. Supercond., 28(3), 2018, 4003806
- T. Gradt, C. Scheuerlein, F. Lackner, F. Savary, "*Friction-coefficient between the Ti6Al4V loading pole and the 316LN steel shims of the HL-LHC 11 T magnets*", IEEE Trans. Appl. Supercond., 28(3), 2018, 4005703.
- U. Kelly, S. Richter, C. Redenbach, K. Schladitz, C. Scheuerlein, F. Wolf, P. Ebermann, F. Lackner, D. Schoerling, D. Meinel, "*3D shape and cross sectional inhomogeneity of Nb_3Sn superconducting wires in Rutherford cables*", IEEE Trans. Appl. Supercond., 28(4), 2018, 4800705.